Interlayer order in illite/smectite

Stephen P. Altaner, Craig M. Bethke

Department of Geology, 1301 West Green Street, University of Illinois, Urbana, Illinois 61801, U.S.A.

Abstract

Interlayer order in interstratified illite/smectite (I/S) has two seemingly contradictory descriptions: the Markov theory developed to explain the X-ray diffraction (xrd) patterns of I/S minerals and the theory of fundamental particles based on observations made by transmission electron microscopy (tem). According to Markov theory, I/S consists of crystallites about 10 nm thick or greater that are composed of stacked illite and smectite interlayers. The stackings are known as MacEwan crystallites. The theory of fundamental particles holds that I/S consists of much smaller crystallites that can accumulate during xrd experiments to give the appearance of MacEwan crystallites.

To test the relationship between the theories, we consider the fundamental-particle content of MacEwan crystallites. In our study we construct synthetic crystallites in which illite and smectite interlayers are arranged by Markov theory. Our results show that Markov theory predicts the size distributions of fundamental particles in randomly interstratified I/S and in I/S with short- and medium-range order. Markov theory, however, poorly predicts tem observations in some illite-rich I/S with long-range order. We suggest that the tem observations complement rather than contradict interpretations of the crystallography of most I/S minerals made on the basis of xrd studies. Apparent discrepancies between the theories can be attributed to the effects of sample preparation for tem experiments.

Introduction

Illite/smectite (I/S) is an interstratified clay mineral of commercial and geologic interest that exhibits properties of both illite and smectite. On the basis of X-ray diffraction (xrd) studies, many petrologists have observed that smectite-rich I/S minerals in sedimentary (Perry and Hower, 1970; Weaver and Beck, 1971; Boles and Franks, 1979) and contact metamorphic (Nadeau and Reynolds, 1981; Pytte, 1982) environments change with time to more illite-rich minerals upon burial and heating. The reaction, termed smectite illitization, can drive petroleum migration (Burst, 1969; Bruce, 1984) and cause geopressures (Powers, 1967; Bethke, 1986) by liberating water from smectite interlayers. The SiO_2, Fe, and Mg produced during smectite illitization are sources of cements in sedimentary rocks (Towe, 1962; Boles and Franks, 1979).

Over the course of the reaction, an xrd peak appears at low values of 2θ and migrates to higher angles. The peak shift signals development of short and then longer ranges of interlayer order (Hoffman and Hower, 1979; Bethke et al., 1986). The type of interlayer order in I/S can be used as an indicator of the thermal histories of sediments and rocks (Hoffman and Hower, 1979; Środoń, 1979; Horton, 1985; Burtner and Warner, 1986).

Interlayer order in I/S has two seemingly contradictory descriptions. Hendricks and Teller (1942) and MacEwan (1956, 1958) introduced Markov theory to study interlayer order in interstratified clays. Their approach considered one-dimensional diffraction from infinitely thick interstratifications of two types of interlayers. Reynolds and Hower (1970) applied Markov theory to calculate xrd patterns in their study of the crystallography of I/S. In their model, I/S is composed of silicate layers about 1 nm thick that are separated by anhydrous illite and hydrous smectite interlayers. The interlayers are arranged along the c* crystallographic axis to form MacEwan crystallites of various ordering types (Zen, 1967).

Interlayer fractions (P_I and P_S) and junction probabilities (e.g., $P_{I \cdot I}$ and $P_{II \cdot I}$) quantify the interlayer order arising within MacEwan crystallites from interactions among neighboring interlayers (Reynolds, 1980). A mineral's Reichweite describes the number of neighbor-to-neighbor interactions that must be considered to model its xrd pattern (Jagodzinski, 1949; Reynolds, 1980). Random interstratifications have a Reichweite of 0 (R0) and show no interactions among neighbors. Reichweite 1 (R1) minerals are ordered by nearest-neighbor interlayers. In minerals with Reichweite 2 and 3 (R2 and R3) order, next-nearest and thrice-removed neighbors further affect interlayer occupancy. Reichweite generally increases with illite content in I/S suites. The Markov description of interlayer interaction provided the basis for previous studies of the thermodynamic properties (Sato, 1965; Zen, 1967) and reaction kinetics (Bethke and Altaner, 1986) of interstratified clay minerals.

Nadeau et al. (1984a, 1984b, 1984c; 1985) and Nadeau (1985) used a Pt-shadowing technique to study dispersed

I/S by transmission electron microscopy (TEM). Their studies showed that I/S is composed of "fundamental particles," each of which is a small but integral number of nanometers thick along c*. The particles are considerably thinner than the crystallite sizes of about 10 to 20 nm commonly inferred from XRD studies. Nadeau et al. proposed that interfaces between fundamental particles can hydrate so that random accumulations of fundamental particles formed during sample preparation for XRD examination can behave as MacEwan crystallites. Interlayers internal to the fundamental particles act as illite, and the hydrous interfaces between particles form smectite interlayers.

The distribution of particle thicknesses provides an alternative description of interlayer order in I/S. In the simplest examples, populations of particles that include only 2-nm-thick particles yield R1-ordered I/S with 50% illite, 3-nm-thick particles yield R2-ordered I/S with 67% illite, and 4-nm-thick particles yield R3-ordered I/S with 75% illite.
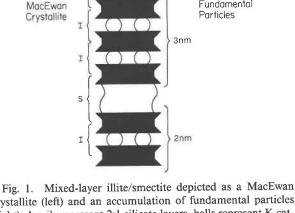
Figure 1 summarizes the relationship between the two theories. On the left, a MacEwan crystallite is represented as six stacked silicate layers. Order type is determined by the arrangement of the five illite and smectite interlayers. On the right, the same crystallite is represented as an accumulation of three fundamental particles. The sizes of the particles determined possible interlayer arrangements.

Previous investigations have emphasized apparent differences between the Markov and fundamental-particle theories (e.g., Klimentidis and Mackinnon, 1986; Ahn and Peacor, 1986). Mackinnon (1987) questioned the precision of measuring fundamental particle thickenesses along the c*-axis with the TEM shadowing method. In this study, we test the relationship of the theories quantitatively. Our calculations show broad agreement between both descriptions of interlayer order for most I/S minerals and help to provide a conceptual link between XRD and TEM experiments.

METHODS

We use a stochastic method to calculate the size distributions of fundamental particles that are predicted by Markov theory to occur within MacEwan crystallites. Our method uses a random-number generator to build a large population of MacEwan crystallites in the memory of a computer. The crystallite interlayers are arranged stochastically according to the illite content and junction probabilities (Reynolds, 1980) of the mineral in question.

Two examples illustrate our technique. In a mineral with 60% illite and random (R0) interstratification, $P_I = P_{I \cdot I} = P_{S \cdot I} = 0.6$. MacEwan crystallites for this mineral are created by choosing illite as the first interlayer in a crystallite 60% of the time and smectite 40% of the time. Succeeding interlayers also have a 60% chance of being set to illite. On the other hand, to build a crystallite with 75% illite interlayers and complete R1 order, the first interlayer has a 75% chance of being set to illite ($P_I = 0.75$). Occupancy of succeeding interlayers depends on the previous interlayer. For R1-ordered I/S, a smectite interlayer is always followed by an illite ($P_{S \cdot I} = 1.0$). An illite interlayer, however, is

Fig. 1. Mixed-layer illite/smectite depicted as a MacEwan crystallite (left) and an accumulation of fundamental particles (right). Anvils represent 2:1 silicate layers, balls represent K cations in illite interlayers, and wavy regions represent water regions that span smectite-interlayer regions.

followed by another illite only 67% of the time because

$$P_{I \cdot I} = 1 - \frac{P_S \cdot P_{S \cdot I}}{P_I} = 0.67$$

(Reynolds, 1980). MacEwan crystallites with longer ranges of order were modeled in the same manner, except that junction probabilities accounting for twice- and thrice-removed neighbors (e.g., $P_{II \cdot I}$ and $P_{III \cdot I}$) were used. Results in this study are based on populations of at least 10000 crystallites, each of which contains 15 interlayers (i.e., 16 silicate layers).

Once a population of crystallites has been constructed, measuring the distances between smectite interlayers gives the sizes of the fundamental particles of which the crystallites are composed. Because the silicate layers (between interlayers) are about 1 nm thick, the separations are integral numbers of nanometers. For example, clay minerals composed entirely of smectite interlayers yield only 1-nm particles, and those with regularly alternating illite and smectite interlayers produce particles 2 nm thick. Clay minerals with more complicated interlayer arrangements give particles in distributions of sizes. Thus, a synthetic size distribution of fundamental particles can be calculated from the probability coefficients of Markov theory.

We applied our technique by analyzing the XRD patterns of I/S minerals. First we determined the Markov coefficients (interlayer fractions and junction probabilities) that best modeled the XRD pattern of each sample studied. In this step, we calculated XRD patterns using a Fourier series technique (Reynolds, 1980; Bethke and Reynolds, 1986) that describes diffraction from oriented clay mounts. We used the resulting interlayer fractions and junction probabilities to calculate the size distribution of fundamental particles for each of the samples, applying the Monte Carlo technique already described. The calculated size distributions allowed us to compare the predictions of Markov theory directly with the TEM observations.

SIMPLE INTERSTRATIFICATIONS

First we consider the interlayer arrangements and fundamental particle contents of simple Markov interstrati-

Random

```
········I·I·I··      ··II··I··I··I···      II··IIIII·I·I·II
·······II··II··      ·I·····I·II···I·      I··III·II······I
·······I····II·      II····II·II···II      I·IIII··II·IIII
·I············      ····II·I···I···I      I··I·I·I·III···
··I····I······      ·I·II·I··I··III       II·III··IIII·II
···I····I·II··      II·III··I·····II      IIII····II··I·I
··II·IIII··I···      I·I·I···II··I·       I·····II·I·I·I
·II······I····      I···II·····II··       I··I··IIII··I··
····I·········      II··I·I··I·I··        ·IIII··I··I··II
I·I········I·I      ··I·····I··I··I       ·I·II·IIIIIIII
```

| 20%   (a) | 40%   (b) | 60%   (c) |

R1-Ordered

```
·I·I·I·I·I·I·       I·I·II·I·I·I·        IIII·I·II·II·I·
·I·I·I·I·I·I·       I·I·I·III·I·II·      I·I·I·I·II·I·II
·I·I·I·I·I·I·       II·I·I·I·I·I·II      II·I·II·II·II·I
·I·I·I·I·I·I·       IIII·I·I·I·I·       III·IIIII·I·I·I
·I·I·I·I·I·I·       I·II·II·I·IIIII      III·II·II·I·I·I
·I·I·I·I·I·I·       I·III·II·II·II·I     I·II·I·II·I·II
I·I·I·I·I·I·I       III·I·II·II·III      I·I·III·I·I·II·
·I·I·I·I·I·I·       I·I·II·I·II·I·I      I·II·I·IIII·III
I·I·I·I·I·I·I       I·I·I·I·I·II·II      ·I·II·II·I·II·I
·I·I·I·I·I·I·       I·I·I·I·II·II·      I·I·I·II·III·II
```

| 50%   (d) | 60%   (e) | 70%   (f) |

R2-Ordered

```
·II·II·II·II·II     ·IIIII·II·III·      III·IIIII·III·I
·II·II·II·II·II     III·IIIIII·II·I     IIII·IIIII·III·
·II·II·II·II·II     ·IIII·II·II·II·     III·IIII·III·II
·II·II·II·II·II     I·II·II·IIIII·I     II·IIIIIIII·III
II·II·II·II·II·     I·III·II·II·II·     IIIIIIIIIII·I
I·II·II·II·II·II    II·II·III·II·II     II·IIIIIII·III
I·II·II·II·II·I     II·II·IIII·III·     II·IIIIII·III·I
I·II·II·II·II·I     III·II·II·II·II     IIIIIIIIIII·II·
·II·II·II·II·II     ·II·II·III·III·     II·IIIII·IIIII
I·II·II·II·II·I     II·IIIIIIII·III·    ·III·II·IIII·II
```

| 67%   (g) | 75%   (h) | 80%   (i) |

R3-Ordered

```
II·III·III·III·     IIII·IIIIII·III     ·IIIIIIIIIIIII
II·III·III·III·     ·IIIII·III·IIII     IIIIII·IIIII·I
II·III·III·III·     I·III·IIIIIIIII     I·IIIIIIIIIIII
·III·III·III·II     ·III·IIIII·III·     ·IIIII·IIIIII·I
II·III·III·III·     II·IIIIIII·III·     IIIII·IIIIIII
II·III·III·III·     II·IIIIIIII·III     IIII·IIII·IIIII
I·III·III·III·I     I·IIIII·III·III     IIIIIIII·IIIII
I·III·III·III·I     I·III·IIIIIIII      IIIIIII·IIIIII
·III·III·III·II     II·IIIII·III·I      IIIIII·IIIIII·
III·III·III·III     I·IIIII·IIII·II     IIIII·IIIIIIII
                    III·III·IIIII·I     I·IIIIII·IIIII
```

| 75%   (j) | 80%   (k) | 90%   (l) |

Fig. 2. Arrangements of smectite and illite interlayers within MacEwan crystallites as predicted by Markov theory for randomly interstratified and R1-, R2-, and R3-ordered I/S with various illite contents. Each row represents a MacEwan crystallite with the crystallographic **c***-axis projected horizontally. I represents an illite and • a smectite interlayer.

fications. Figure 2 shows typical structures of MacEwan crystallites over the range of compositions and ordering types commonly observed in natural I/S. The crystallites were constructed stochastically using the Monte Carlo method. In I/S with random interstratification and containing 20, 40, and 60% illite (Figs. 2a, 2b, and 2c), clustering (e.g., SSS··· or III···) and alternation (ISISIS···) of interlayers are apparent in the synthetic crystallites. Illite interlayers have a greater tendency to form clusters as illite content increases, so that clusters of more than

several interlayers are common in the crystallites containing 60% illite. Disarticulating the crystallites at smectite interlayers, each cluster would form a fundamental particle whose thickness in nanometers is the number of illite interlayers in the cluster plus one.

Figures 2d–2f show typical interlayer arrangements of I/S with complete R1 ordering and illite contents of 50, 60, and 70%. In the case of half illite interlayers, all of the crystallites appear in the regular alternation (ISISIS ···) characteristic of rectorite. As illite content increases, however, alternations become less dominant and illite clusters more common. There are no clusters of smectite interlayers because $P_{S-S} = 0$ in R1-ordered I/S. Notably, R1-ordered I/S with 70% illite, a common interstratification in nature, has little tendency for interlayer alternations of more than two cycles. For example, the possibility of encountering six interlayers in the triple alternation ISISIS (or its inverse) in this mineral is about 1%. Thus, this mineral would not resemble rectorite in lattice-fringe images although both minerals have the same type of ordering and similar illite contents.

In a comparable manner, R2-ordered I/S composed of 67% illite (Fig. 2g) and R3-ordered I/S with 75% illite (Fig. 2j) show ordered arrangements in which smectite interlayers are separated by 2 or 3 illite interlayers, respectively. I/S with illite contents greater than these examples (Figs. 2h, 2i, 2k, 2l), however, shows progressive loss of the alternation structure of the end members and development of interlayer clusters that dominate the crystallite structures.

Calculated interlayer arrangements such as those in Figure 2 can be compared with the interlayer arrangements observed in high-resolution TEM investigations. Both clustering and alternation have been observed in lattice-fringe images of I/S minerals that have been treated chemically to hold smectite interlayers expanded under vacuum (Klimentidis and Mackinnon, 1986; Ahn and Peacor, 1986; Vali and Koster, 1986). Calculated structures should prove useful for interpreting the results of such experiments.

Figure 3 shows the size distributions of fundamental particles in I/S of the ordering types and illite contents considered in Figure 2. The size distributions were determined by measuring the distances between smectite interlayers in 10000 crystallites with stochastically determined interlayer arrangements. Randomly interstratified I/S is composed of particles over a range of sizes. The range of sizes and the number of particles more than several nanometers thick increase with illite content. The thicker particles appear in Figure 2c as clusters of illite interlayers.

R1-, R2-, and R3-ordered I/S minerals with 50, 67, and 75% illite, however, contain fundamental particles of a single size within crystallite interiors. Combining these particles gives the regular interlayer arrangements of ISIS ···, IISIIS···, and IIISIIIS··· that appear in Figure 2. The minerals also contain smaller particles that appear only at the ends of crystallites. These particles occur be-
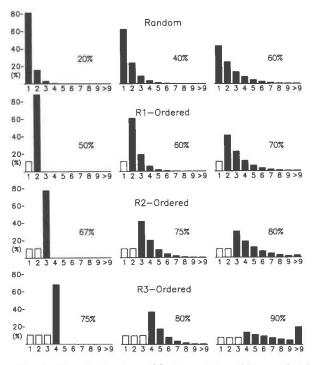
Fig. 3. Size distributions of fundamental particles predicted by Markov theory for randomly interstratified and R1-, R2-, and R3-ordered I/S with various illite contents. By Markov theory, most I/S minerals contain a distribution of particle sizes. Sizes are in nanometers and represent the number of illite interlayers along c^* within a particle. Open bars represent particles occurring at crystallite ends.

Fig. 4. Observed XRD pattern for ethylene glycol–solvated sample WWB (Nadeau et al., 1985) with observed size distribution of fundamental particles (top), and calculated XRD pattern for I/S with 30% illite and random interstratification, with particle-size distribution resulting from Markov theory (bottom). Peak spacings on XRD patterns are given in nanometers.

cause the synthetic MacEwan crystallites contain a fixed number of interlayers. Markov theory describes finite series within infinitely long sequences and was applied exactly in Hendricks and Teller's (1942) study of infinitely thick crystallites. Reynolds and Hower (1970) and Reynolds (1980) modified the theory slightly to describe interlayer arrangements within the finite sequences that make up MacEwan crystallites. In our analysis, assuming interlayer sequences of finite length results in the possibility that truncated fundamental particles can occur at the ends of crystallites. Particles that occur only at crystallite ends are shown by open bars in Figure 3.

As illite content increases from the end-member cases presented, particle sizes fall in increasingly broad distributions. The breadth of the distributions represents increasing likelihood of encountering clusters of illite interlayers within ordered MacEwan crystallites. Thus, even I/S with complete short- or long-range ordering, except in end-member cases requiring perfect alternation, contains fundamental particles of a variety of thicknesses.

ANALYSIS OF NATURAL SAMPLES

We applied our method of analysis to a suite of I/S minerals studied by Nadeau et al. (1985). The suite contains samples WWB, CCB, NCB, LPB, RAN, and TGB, which effectively span the range of I/S compositions and
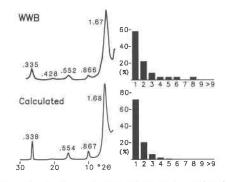
ordering types common in nature. Nadeau et al. (1985) measured the thicknesses of between 22 and 78 fundamental particles from each sample. To analyze these samples, we determined the interlayer fractions and junction probabilities that gave the calculated XRD patterns that most closely matched the actual patterns of the I/S minerals (Table 1). We used these values to synthesize interlayer arrangements in MacEwan crystallites and the corresponding particle-size distributions, using the Monte Carlo technique. We then compared the calculated distributions to the distributions determined by TEM measurement.

Figure 4 shows XRD patterns and size distributions of fundamental particles for sample WWB, a Cretaceous bentonite from Westwater, Utah. WWB contains about 30% illite and is typical of randomly interstratified I/S. The top of the figure shows the observed XRD pattern and measured distribution of particle sizes. The bottom of the figure shows the calculated XRD pattern that best matches the observed pattern and the synthetic particle-size distribution.

The calculated distribution predicts predominance of 1-nm particles, and significant numbers of 2 nm and 3 nm particles, in good agreement with the observed distribution. Small differences between the calculated and observed data—such as the slight depletion of thin particles and enrichment of thick ones in the observations

TABLE 1. Predominant ordering type (Reichweite), illite interlayer fractions, and junction probabilities for samples analyzed

Sample	Ordering type	P_I	P_{II-I}	P_{III-I}	P_{IIII-I}
WWB	R0	.3			
NCB	R0–R1	.55	.38		
CCB	R0–R1	.5	.25		
LPB	R1–R2	.75	.67	.63	
RAN	R3	.90	.89	.88	.86
TGB	R3	.90	.89	.88	.86

Fig. 5. Arrangements of interlayers (a) calculated stochastically on the basis of Markov theory and (b) random accumulations of fundamental particles for sample WWB.

Fig. 7. Arrangements of interlayers (a) calculated on the basis of Markov theory and (b) random accumulations of fundamental particles for sample NCB.

relative to the calculations—are not statistically significant because of the relatively small number of measurements. For example, one particle was observed for each thickness of 4, 5, 6, and 8 nm. Each of these particles represents about 3% of the total population, a somewhat greater fraction than is predicted by the calculated distributions. On the basis of counting theory (e.g., Bertin, 1978), however, each of these measurements carries a standard deviation of 100% of the observed value. For this reason, discrepancies here are not necessarily significant.

Figure 5 shows interlayer arrangements in random MacEwan crystallites, calculated from Markov theory as described before, and those that would result from accumulation of fundamental particles from the measured population. In the latter case, a computer randomly chose particles and added them to an accumulation one at a time until the accumulation contained more than 10 interlayers. Interlayers internal to the particles form illites and the interfaces between the accumulated particles make up smectite interlayers. The representations are similar, showing common clusters of both illite and smectite interlayers. Illite clusters are somewhat more common in the random accumulations because the four particles >3

nm in thickness make up >10% of the population of observed particles (and a considerably greater share of the population's volume).

Sample NCB (Fig. 6), a Cretaceous bentonite from New Castle, Colorado, is representative of I/S with short-range order. The XRD pattern of this sample is best modeled assuming a composition of 55% illite and incomplete R1 order. The calculated size distribution predicts that 2-nm particles are predominant and that significant numbers of particles 1 nm and >3 nm thick occur. Except for some inflation of the population at 1 nm due to crystallite-end effects, the calculated and observed distributions match closely. Synthetic interlayer arrangements (Fig. 7a) show a greater tendency for interlayer alternation than the previous sample. The synthetic arrangements clearly resemble those that would result from the accumulation of fundamental particles (Fig. 7b). Sample CCB (data not shown), a Cretaceous bentonite from Canon City, Colorado, is also representative of I/S with short-range order. The XRD pattern of this sample is best modeled assuming a composition of 50% illite and incomplete R1 order. In this sample, agreement between Markovian predictions and TEM observations is similar to that observed for sample NCB.
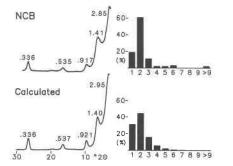

Fig. 6. Mineralogical observations for sample NCB (Nadeau et al., 1985) as described for Fig. 4 (top), and predictions of Markov theory for I/S with 55% illite and 45% R1 order (bottom).
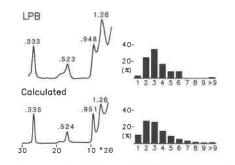

Fig. 8. Mineralogical observations for sample LPB (Nadeau et al., 1985) as described for Fig. 4 (top), and predictions of Markov theory for I/S with 75% illite, complete R1 order, and 25% R2 order (bottom).

```
·II·II·II·IIIII          II·IIIII·III
IIIII·I·IIIIII·          IIIII·III·II
III·III·I·II·I·          II·I·III·I·II
I·I·IIIII·IIIII          I·I·I·I·I·IIIII
I·III·I·IIIII·I          I·IIII·III·III
·IIIIIIII·IIII·          II·IIIII·III
II·II·II·IIIIII          II·II·II·IIIII
II·IIII·III·III          II·I·IIIII·II
IIIIII·III·I·I·          III·I·I·I·II
IIII·I·III·III·I         II·II·IIIII
II·IIIIIII·I·II          I·I·II·I·I·I
I·IIII·II·IIIII          II·II·III·III
·II·IIIII·III·II         IIII··II·II
I·IIIIII·IIIII·          IIII·III·II
        (a)                 (b)
```

Fig. 9. Arrangements of interlayers (a) calculated on the basis of Markov theory and (b) random accumulations of fundamental particles for sample LPB.
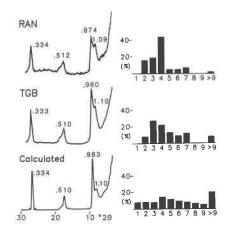

Fig. 10. Mineralogical observations of samples RAN and TGB (Nadeau et al., 1985) as described for Fig. 4 (top), and predictions of Markov theory for I/S with 90% illite and complete R3 order (bottom). The observed and predicted size distributions are qualitatively different.

Sample LPB (Fig. 8), a Cretaceous bentonite from Las Piedras, Colorado, is typical of I/S with short- to intermediate-range order. The XRD pattern of this sample is best modeled assuming 75% illite with complete R1 order and partial R2 order. The corresponding size distribution predicts a broad distribution of particle sizes with 2-nm and 3-nm particles in greatest abundance. Significant clustering of illite interlayers and some alternation are predicted (Fig. 9a). Again, the Markovian predictions compare well with the observed size distribution and calculated interlayer arrangements, except for some inflation of 1-nm and 2-nm populations due to the effects of assuming fixed crystallite sizes.

Samples RAN (a Permian sandstone from the southern North Sea basin) and TGB (a Devonian bentonite from Mohawk Valley, New York) are typical of I/S with long-range order (Fig. 10). The XRD patterns for these samples are best modeled assuming 90% illite with complete R3 order. Calculated XRD patterns, however, fail to model the observed patterns exactly. In particular, significant differences occur in the diffracted intensity near 1.1 and 0.48 nm.

Markov theory predicts size distributions for samples RAN and TGB that are qualitatively different from the observed distributions. Whereas the calculated distribution predicts numerous particles >7 nm thick, such particles are rare in TGB or RAN. In addition, these samples contain significant populations of 2- and 3-nm particles, whereas these particles occur only at the ends of MacEwan crystallites ordered by Markov theory. Calculated MacEwan crystallites (Fig. 11a) contain longer and more abundant clusters of illite interlayers than arrangements calculated from size distributions of fundamental particles (Fig. 11b). Apparently, Markov theory, which has not been completely successful in describing XRD patterns of I/S minerals with long-range order (Reynolds, 1980, p. 297), cannot predict even qualitatively the TEM observations of these minerals.

INTERLAYER CONTENT OF I/S

To test further the relationship between the Markov model and the concept of fundamental particles, we compare the estimate of the fraction of illite interlayers in I/S (P_I) resulting from Markov analysis of XRD patterns to the interlayer content of accumulations of fundamental particles. The latter can be calculated directly from measured size distributions of fundamental particles.

Consider a population of N_t particles of known thickness. There are N_1 particles 1 nm thick, N_2 particles 2 mm thick, and so on, so that

$$N_t = \sum_i N_i.$$

MacEwan crystallites are stacked arrangements of the particles. Within the crystallites, illite interlayers are internal to the particles, and smectite interlayers occur at the interfaces between particles. Arranging the N_t particles into N_x MacEwan crystallites, then,

$$n_t = N_1 + 2N_2 + 3N_3 + \cdots - N_x$$
$$= \sum_i iN_i - N_x,$$

where n_t is the total number of interlayers. N_x is subtracted from the summation because there is one fewer interlayer than silicate layer in each crystallite.

Of the total number of interlayers,

$$n_I = N_2 + 2N_3 + 3N_4 + \cdots$$
$$= \sum_i (i - 1)N_i$$

are illite interlayers. The interlayer fraction P_I(f.p.) is the ratio of the number of illite to total interlayers determined on the basis of the size distributions of fundamental particles for the samples in question:

$$P_I \text{ (f.p.)} = \frac{n_I}{n_t} = \frac{\sum_i (i - 1)f_i}{\sum_i if_i - 1/N_p}. \tag{1}$$

```
IIIII·IIIIIIIII          IIIIIIIIIIIII
IIIIIIIIII·IIII          IIIII·IIII
IIIIIII·IIIIIII          IIIII·IIIIII
IIIIIIIIIIIIII·          II·IIIIII·III
II·IIIII·III·II          II·II·IIII·II
IIIIII·IIIIIII           III·III·IIIII
IIIII·IIIIIIII           IIIII·IIII·I
I·IIII·IIIIIII           I·I·III·III
III·III·IIIIII           IIIIIIIIIIIII
IIIIIIIIIIIIII           IIIII·IIIIII
IIIIIIIIIIIIII           IIIII·I·III
IIII·IIIIIIII·           II·IIIII·II
IIIIII·IIII·III          III·IIIII·III
IIIII·IIIIIIIII          II·IIII·II·III

     (a)                     (b)
```

Fig. 11. Arrangements of interlayers (a) calculated on the basis of Markov theory and (b) random accumulations of fundamental particles for sample TGB.

Here, f_i is the fraction N_i/N_t of particles i nm thick, and N_p is the average number of particles N_t/N_x per crystallite. This equation is similar to Equation 1 in Eberl et al. (1987) and the equations on p. 508 in Nadeau (1985), except for the $1/N_p$ term that accounts for the finite number of particles constituting a crystallite. Equation 1 gives interlayer fractions directly from the particle-size distributions f_i determined by TEM experiments.

Figure 12 shows the relationship of P_I (f.p.) given by Equation 1 from measured particle-size distributions with P_I (Markov) estimated by modeling the XRD patterns of the samples studied. Values agree well for I/S and R1- and R2-ordering types (samples CCB, NCB, and LPB). This correlation argues that Markov theory accurately describes interlayer abundances in this type of I/S. Sample WWB, which has R0 order, gives a value of P_I (f.p.) significantly greater than P_I (Markov). We suggest that this discrepancy is due to the overestimate of large particles, which might be more easily imaged by shadowing techniques. For example, ignoring the four measured particles >3 mm thick in this sample (a total of 12% of the measured population) gives near perfect agreement, as shown by the open circle in Figure 12.

For sample TGB, P_I (Markov) > P_I (f.p.) and for sample RAN, P_I (Markov) ≫ P_I (f.p.). Notably, these two samples have XRD patterns and distributions of fundamental particles that are poorly modeled by Markov theory. These differences in determination of interlayer content are consistent with our suggestion that Markov theory poorly describes the structure of I/S with interpreted long-range order.

DISCUSSION

Results in this study show broad agreement between the predictions of Markov theory and the observed size distributions of fundamental particles for I/S with random and short ranges of interlayer order. This agreement indicates that the precision of the TEM technique is adequate for measuring c*-axis thicknesses of Pt-shadowed samples, despite the concerns raised by Mackinnon (1987). On this basis, we conclude that TEM measurement of the thicknesses of fundamental particles for these minerals
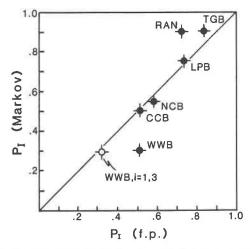

Fig. 12. Fraction of illite interlayers in I/S for samples analyzed. Illite contents are from analysis of XRD patterns using Markov theory P_I (Markov) and calculations based on the size distributions of fundamental particles P_I (f.p.) according to Equation 1. Closed symbols represent illite contents based on measurements of fundamental-particle size. Open symbol for WWB represents an illite content calculated on the basis of populations of particles 1 to 3 nm thick.

support rather than contradict interpretations of interlayer order made on the basis of XRD studies.

Markov theory, however, cannot explain the abundance of particles <4 nm thick and the paucity of particles >7 nm thick in illite-rich I/S intepreted to have long-range (R3) order. On the basis of the relative abundances of 5-nm to 7-nm particles in samples RAN and TGB, illite-rich I/S might contain especially long ranges of ordering (R4–R6), which are difficult to describe using current formulations of Markov theory. The significant number of particles just 2 and 3 nm thick in these samples suggests that the very long range order would be incomplete. Lattice-fringe imaging of illite-rich I/S should provide important insights into the nature of these minerals.

An unresolved question is whether Markov theory or the fundamental-particle concept best describes the crystallite sizes of I/S minerals in nature. MacHardy et al. (1982) estimated crystallite thicknesses of filamentous I/S from sandstone pores using scanning electron microscopy. They concluded that these clays have thicknesses more similar to fundamental particles than to MacEwan crystallites. Lattice-fringe images of I/S from bentonites, however, show crystallites that are closer in thickness to MacEwan crystallites than to fundamental particles (Lee and Peacor, 1986; Vali and Koster, 1986; Klimentidis and Mackinnon, 1986). Sampling bias, however, could account for the lack of published lattice-fringe images of fundamental particles. For example, dispersed fundamental particles may be difficult to image because of their small thicknesses.

These observations might be reconciled if smectite interlayers disarticulate by osmotic swelling after the Na-

or Li-saturation process used in preparing samples for Pt-shadowing analysis. Osmotic swelling might cause MacEwan crystallites to cleave along smectite interlayers. Ahn and Peacor (1986) made a similar suggestion, although they proposed that large MacEwan crystallites cleave along smectite interlayers because of grinding during sample preparation rather than osmotically. Several studies have shown that water-rich suspensions of smectite exchanged with Li and Na dissociate into individual 1-nm-thick particles (Norrish, 1954; Foster et al., 1955; Suquet et al., 1975), although the degree of dissociation is reduced as salinity increases (Norrish and Rausell-Colom, 1963). Disarticulation arises from the large hydration energies of Na and Li cations and from the greater salinities in the interlayers relative to the solutions used in sample preparation.

Because Ca, Mg, K, and Ba ions have low hydration energies, smectites saturated with these cations do not exhibit significant osmotic swelling (Suquet et al., 1975). Disarticulation into fundamental particles would not be expected under these conditions. This observation may explain why dispersed samples of untreated I/S show larger values of mean particle thickness (Inoue et al., 1987) than Li- or Na-exchanged I/S with the same illite content (Nadeau et al., 1985). Apparently, the untreated samples retain poorly hydrated ions such as Ca in their interlayers and do not disarticulate completely. Because these cations are abundant in most groundwaters, I/S may also be relatively articulated in nature.

In the laboratory, disarticulation seems to be sufficiently reversible to reform MacEwan crystallites upon drying when the clay is dispersed in dilute solutions. For example, Nadeau et al. (1984a, 1984b, 1984c, 1985) observed that accumulations of fundamental particles from Na- and Li-exchanged I/S appear as MacEwan crystallites in XRD experiments, giving rise to their interpretation of interparticle diffraction. From these considerations, we propose that osmotic swelling could explain the apparent dual nature of I/S: the thin particles observed in Pt-shadowing experiments after dispersion in Na and Li solutions and the thicker crystallites observed in XRD experiments and lattice-fringe images.

ACKNOWLEDGMENTS

REFERENCES CITED

Ahn, J.H., and Peacor, D.R. (1986) Transmission electron microscope data for rectorite: Implications for the origin and structure of "fundamental particles." Clays and Clay Minerals, 34, 180–186.
Bertin, E.P. (1978) Introduction to X-ray spectrometric analysis, p. 299–310. Plenum Press, New York.
Bethke, C.M. (1986) Inverse hydrologic analysis of the distribution and origin of Gulf Coast–type geopressured zones. Journal of Geophysical Research, 91, 6535–6545.
Bethke, C.M., and Altaner, S.P. (1986) Layer-by-layer mechanism of smectite illitization and application to a new rate law. Clays and Clay Minerals, 34, 136–145.
Bethke, C.M., and Reynolds, R.C. (1986) Recursive method for determining frequency factors in interstratified clay diffraction calculations. Clays and Clay Minerals, 34, 224–226.
Bethke, C.M., Vergo, N., and Altaner, S.P. (1986) Pathways of smectite illitization. Clays and Clay Minerals, 34, 125–135.
Boles, J.R., and Franks, S.G. (1979) Clay diagenesis in Wilcox sandstones of southwest Texas: Implications of smectite diagenesis on sandstone cementation. Journal of Sedimentary Petrology, 49, 55–70.
Bruce, C.H. (1984) Smectite dehydration, its relation to structural development and hydrocarbon accumulation in northern Gulf of Mexico Basin. American Association of Petroleum Geologists Bulletin, 68, 673–683.
Burst, J.F. (1969) Diagenesis of Gulf Coast clayey sediments and its possible relation to petroleum migration. American Association of Petroleum Geologists Bulletin, 53, 73–93.
Burtner, R.L., and Warner, M.A. (1986) Relationship between illite/smectite diagenesis and hydrocarbon generation in Lower Cretaceous Mowry and Skull Creek shales of the northern Rocky Mountain area. Clays and Clay Minerals, 34, 390–402.
Eberl, D.D., Środoń, J., Lee, M., Nadeau, P.H., and Northrop, H.R. (1987) Sericite from the Silverton caldera, Colorado: Correlation among structure, composition, origin, and particle thickness. American Mineralogist, 72, 914–934.
Foster, W.R., Savins, J.G., and Waite, J.M. (1955) Lattice expansion and rheological behavior relationships in water-montmorillonite systems. Clays and Clay Minerals, 3, 296–316.
Hendricks, S.B., and Teller, E. (1942) X-ray interference in partially ordered layer lattices. Journal of Chemical Physics, 10, 147–167.
Hoffman, J., and Hower, J. (1979) Clay mineral assemblages as low-grade metamorphic geothermometers: Application to the thrust faulted disturbed belt of Montana, USA. Society of Economic Paleontologists and Mineralogists Special Paper 26, 55–79.
Horton, D.G. (1985) Mixed-layer illite/smectite as a paleotemperature indicator in the Amethyst vein system, Creede district, Colorado, USA. Contributions to Mineralogy and Petrology, 91, 171–179.
Inoue, A., Kohyama, N., Kitagawa, R., and Watanabe, T. (1987) Chemical and morphological evidence for the conversion of smectite to illite. Clays and Clay Minerals, 35, 111–120.
Jagodzinski, H. (1949) One dimensional disorder in crystals and their influence on x-ray interferences: I. Calculation of the degree of disorder from the x-ray intensities. Acta Crystallographica, 2, 201–207 (in German).
Klimentidis, R.E., and Mackinnon, I.D.R. (1986) High-resolution imaging of ordered mixed-layer clays. Clays and Clay Minerals, 34, 155–164.
Lee, J.H., and Peacor, D.R. (1986) Expansion of smectite by laurylamine hydrochloride: Ambiguities in transmission electron microscope observations. Clays and Clay Minerals, 34, 69–73.
MacEwan, D.M.C. (1956) Fourier transform methods for studying scattering from lamellar systems: I. A direct method for analyzing interstratified mixtures. Kolloidzeitschrift, 149, 96–108.
——— (1958) Fourier transform methods for studying X-ray scattering from lamellar systems: II. The calculation of X-ray diffraction effects for various types of interstratification. Kolloidzeitschrift, 156, 61–67.
Mackinnon, I.D.R. (1987) The fundamental nature of illite/smectite mixed-layer clay particles: A comment on papers by P.H. Nadeau and co-workers. Clays and Clay Minerals, 35, 74–76.
McHardy, W.J., Wilson, M.J., and Tait, J.M. (1982) Electron microscope and X-ray diffraction studies of filamentous illitic clay from sandstones of the Magnus field. Clay Minerals, 17, 23–39.
Nadeau, P.H. (1985) The physical dimensions of fundamental clay particles. Clay Minerals, 20, 499–514.
Nadeau, P.H., and Reynolds, R.C. (1981) Burial and contact metamorphism in the Mancos shale. Clays and Clay Minerals, 29, 249–259.
Nadeau, P.H., Tait, J.M., McHardy, W.J., and Wilson, M.J. (1984a) Interstratified XRD characteristics of physical mixtures of elementary clay particles. Clay Minerals, 19, 67–76.
Nadeau, P.H., Wilson, M.J., McHardy, W.J., and Tait, J.M. (1984b) Interstratified clays as fundamental particles. Science, 225, 923–925.

———(1984c) Interparticle diffraction, a new concept for interstratified clays. Clay Minerals, 19, 757–769.

———(1985) The conversion of smectite to illite during diagenesis: Evidence from some illitic clays from bentonites and sandstones. Mineralogical Magazine, 49, 393–400.

Norrish, K. (1954) The swelling of montmorillonite. Transactions of the Faraday Society, 18, 120–134.

Norrish, K., and Rausell-Colom, J.A. (1963) Low angle X-ray diffraction studies of the swelling of montmorillonite and vermiculite. Clays and Clay Minerals, 10, 123–149.

Perry, E., and Hower, J. (1970) Burial diagenesis in Gulf Coast pelitic sediments. Clays and Clay Minerals, 18, 165–177.

Powers, M.C. (1967) Fluid-release mechanisms in compacting marine mudrocks and their importance in oil exploration. American Association of Petroleum Geologists Bulletin, 51, 1240–1254.

Pytte, A.M. (1982) The kinetics of the smectite to illite reaction in contact metamorphic shales, 78 p. M.A. thesis, Dartmouth College, Hanover, New Hampshire.

Reynolds, R.C. (1980) Interstratified clay minerals. In G.W. Brindley and G. Brown, Eds., Crystal structures of clay minerals and their X-ray identification, p. 249–303. Mineralogical Society, London.

Reynolds, R.C., and Hower, J. (1970) The nature of interlayering in mixed-layer illite-montmorillonites. Clays and Clay Minerals, 18, 25–36.

Sato, M. (1965) Structure of interstratified (mixed-layer) minerals. Nature, 208, 70–71.

Środoń, J. (1979) Correlation between coal and clay diagenesis in the Carboniferous of the Upper Silesian coal basin. Proceedings of the International Clay Conference, Oxford, 251–260.

Suquet, H., De La Calle, C., and Pezerat, H. (1975) Swelling and structural organization of saponite. Clays and Clay Minerals, 23, 1–9.

Towe, K.M. (1962) Clay mineral diagenesis as a possible source of silica cement in sedimentary rocks. Journal of Sedimentary Petrology, 32, 26–28.

Vali, H., and Koster, H.M. (1986) Expanding behavior, structural disorder, regular and random irregular interstratification of 2:1 layer-silicates studied by high-resolution images of transmission electron microscopy. Clay Minerals, 21, 827–859.

Weaver, C.E., and Beck, K.C. (1971) Clay water diagenesis during burial: How mud becomes gneiss. Geological Society of America Special Paper 134, 96 p.

Zen, E.-A. (1967) Mixed-layer minerals as one-dimensional crystals. American Mineralogist, 52, 635–660.